Scientific Journal of Engineering, and Technology (SJET)

ISSN: 3007-9519 (Online)

Volume 2 Issue 1, (2025)

https://doi.org/10.69739/sjet.v2i1.553

https://journals.stecab.com/sjet

Published by
Stecab Publishing

Research Article

Performance Optimization of Wet Turning of Aluminum Alloy 6351 Eggshell Reinforced Composite Using Response Surface Methodology

*[1]Bethel Mba, [2]S. C. Nwoziri, [3]Franklin Onwuka, [4]Uchenna Alozie, [5]L. J. King, [6]Onyekachi Monday Okafor

About Article

Article History

Submission: April 09, 2025
Acceptance : May 14, 2025
Publication : May 22, 2025

Keywords

Material Removal Rate, Numerical Optimization, Regression Equation, Response Surface Methodology, Surface Roughness

About Author

[1] Department of Mechanical Engineering, Michael Okpara University of Agriculture Umudike, Nigeria

[2] Department of Mechanical Engineering, University of Calabar, Nigeria

[3] Department of Mechanical Engineering, Federal University of Nigeria Nsukka, Nigeria

[4] Department of Mechanical Engineering, Federal Polytechnic Nekede, Nigeria

[5] Department of Mechanical Engineering, Federal University of Technology Owerri, Nigeria

[6] Department of Mechanical Engineering, University of Chester, United Kingdom

Contact @ Bethel Mba
mbabethelchidiadi@gmail.com

ABSTRACT

The limited understanding of key input parameters and material machinability has hindered the industry's full utilization of machining processes. These limitations make it challenging to meet machining response requirements and address various related issues. This study employs Response Surface Methodology (RSM) to explore the interaction between input parameters and responses during the wet turning of aluminum alloy eggshell reinforced composite (AAERC). Numerical optimization was used to determine the optimal combinations of process parameters, achieving the best results in terms of Material Removal Rate (MRR) and Surface Roughness (Ra). The AAERCs consisted of 85% aluminum alloy and 15% eggshell. To enhance wettability, 2% of equal-sized crushed magnesium powder was added to the molten metal. Improved wettability decreases surface tension, increases surface energy, and reduces the energy at the matrix-reinforcement interface. The developed regression equation model can predict Ra and MRR when input variables such as cutting speed (V_C), feed rate (F_r), and depth of cut (D_C) are known. The fit statistics for MRR and Ra indicate that the R^2 and adjusted R^2 values are 0.9461 and 0.8490 for Ra, and 0.9745 and 0.9286 for MRR, respectively. These values demonstrate that the models provide a strong fit for both responses. The parameters V_C, F_r and D_C, with P-values of 0.0003, 0.0017, and 0.0008 respectively, significantly influence MRR. Similarly, V_C and F_r, with P-values of 0.0006 and 0.0583 respectively, significantly impact Ra. The optimization process results indicate that the optimal values for Ra and MRR are 1.0689μm and 1793.93mm³/min, respectively. These results are achieved when turning operations on AAERC are conducted using the input variables V_C, D_C, and F_r at 369.822rpm, 0.333554mm/min, and 0.235944mm, respectively.

Citation Style:

Mba, B., Nwoziri, S. C., Onwuka, F., Alozie, U., King, L. J., & Okafor, O. M. (2025). Performance Optimization of Wet Turning of Aluminum Alloy 6351 Eggshell Reinforced Composite Using Response Surface Methodology. *Scientific Journal of Engineering, and Technology, 2*(1), 112-125. https://doi.org/10.69739/sjet.v2i1.553

1. INTRODUCTION

The manufacturing industry aims to produce a variety of items in small batches at low costs while increasing production volumes in today's competitive market (Edh Mirzaei *et al*., 2021). Machining involves removing excess material or metal from a workpiece using a cutting tool (Mba *et al*., 2024). This subtractive manufacturing method shapes the desired end product by precisely removing unwanted material, optimizing tool life, and achieving a smooth surface finish (Nwoziri *et al*., 2024).

Machining is the most effective method for creating components with precise tolerances (Subbiah, 2014). Turning is a metal-cutting process used to shape cylindrical objects by rotating a workpiece on a lathe while a cutting tool removes material. This method provides shorter lead times and smoother surface finishes (Krajčoviech *et al*., 2021; Guleria *et al*., 2023; Karmiris-Obratanski *et al*., 2024). It is the most widely used machining process globally, with increasing adoption due to continuous technological advancements in lathe systems (Joshi & Kumar, 2021; Kaniapan *et al*., 2022). Efficient and economical machining aims for quick material removal, low power consumption, ideal dimensional accuracy and quality, reduced tool costs, and minimal idle time (Lv *et al*., 2021; Sun *et al*., 2021). However, inadequate parameters can hinder even the most intricate and comprehensive machining procedures from yielding meaningful results (Maurya & Niranjan, 2024; Mohanta *et al*., 2024). Therefore, it is crucial to control the many input parameters that affect the output's reactions (Jain *et al*., 2023; Jiang *et al*., 2018).

The material produced during machining is significantly influenced by the cutting parameters used (Abellán-Nebot *et al*., 2024). Optimizing these parameters can yield the best results while minimizing resource waste and costs (Udaya Prakash *et al*., 2022). Higher material removal rates, longer tool life, and better surface finishes are essential throughout the machining process (Seenath & Sarhan, 2024). The goal in selecting control variables is to mitigate the impact of disruptive elements (Pawanr & Gupta, 2024). Key factors determining the effectiveness and quality of lathe turning operations include depth of cut, feed rate, cutting speed, rake angle, workpiece size, tool geometry, material type, tool vibration, and lubricant type (Jia *et al*., 2021). High cutting speeds, feed rates, and depths of cut are necessary for greater material removal rates; however, these combinations generate significant heat at the cutting zone, negatively affecting surface quality, dimensional accuracy, and tool life (Li *et al*., 2024; Tefera *et al*., 2023; Thanh *et al*., 2024). Material Removal Rate (MRR) is a crucial metric in machining processes, indicating how much material is removed over a specific time period (Deresse *et al*., 2020). It is vital for assessing the effectiveness of processes like drilling, grooving, milling, and turning (Kumar *et al*., 2023).

Eggshell powder can significantly influence Material Removal Rate (MRR) and surface roughness in machining processes. Adding eggshell powder to composite materials or using it as a reinforcement in machining can improve mechanical properties and enhance surface finish (Li *et al*., 2021). For instance, eggshell powder can act as a natural abrasive, improving the MRR by facilitating more efficient material removal. Additionally, its fine particles can help achieve a smoother surface finish by reducing surface irregularities during the machining process (Li *et al*., 2021). Overall, the use of eggshell powder in machining applications can lead to better performance, higher efficiency, and improved surface quality.

The surface roughness profile of a product is influenced by friction, wear rate, and lubricant type. Developing and validating a mathematical model is essential to predict responses considering all machining input variables (Wang *et al*., 2024; Yan *et al*., 2023). Surface texture control and dimensional precision have become crucial in modern engineering processes and products (Soni *et al*., 2024). Surface roughness significantly impacts the performance of machined goods. Achieving a completely smooth surface is impossible, regardless of the manufacturing process used (Abellán-Nebot *et al*., 2024). Surface roughness refers to the imperfections on machined material surfaces, characterized by a unidirectional and evenly spaced pattern from machining processes. Key factors affecting surface roughness include vibrations, workpiece material, machining type, system rigidity, cutting tool type, and cutting parameters (Zheng *et al*., 2020).

Aluminum, magnesium, and titanium alloys serve as matrix materials in Metal Matrix Composites (MMC) (Raja & Gupta 2021). Reinforcement components in MMCs include oxides, carbides, and borides, which can be in the form of long or short fibers (whiskers) (Wong & Seetharaman, 2021). Aluminum alloys and composites are favored in the automotive and aerospace industries due to their low weight, easy availability, corrosion resistance, and high strength-to-weight ratios (Khan *et al*., 2024). However, improper execution of Aluminum Metal Matrix Composite (AMMC) machining operations can lead to defects such as dimetral variation, poor Material Removal Rate (MRR), and negative surface roughness (Kotteda *et al*., 2022). The presence of reinforcement significantly affects the machinability of composites, with the volume percentage and size of the reinforcement playing crucial roles in determining how easily composite materials can be machined (Chen *et al*., 2020; Gasha *et al*., 2024).

The machining process is intricate and influenced by numerous factors, making it challenging for operators to achieve optimal performance (Jiang *et al*., 2024). To mathematically describe and optimize the process, it is crucial to link process outputs with input parameters and use the appropriate optimization techniques. This paper focuses on optimizing the performance of wet turning of aluminum alloy 6351 reinforced with eggshell composite using response surface methodology. The primary aim of this study is to identify the optimal cutting parameters for wet turning of aluminum alloy 6351 reinforced with eggshell composite.

2. LITERATURE REVIEW

Aluminum metal matrix composites (AMMCs) are produced to almost net shape and often need to be machined to improve performance and productivity (Kumar *et al*., 2024; Tiwari & Yadav, 2024). Machining properties are influenced by the volume proportion of the reinforcement and matrix, the kind of reinforcement (particle or whisker), the distribution of reinforcement in the matrix, and the reinforcement material. AMMC machining yields different results than metal machining because of the strong and brittle reinforcing (Jain *et al*., 2014).

Conversely, the cutting tool comes into contact with matrix and reinforcing materials, each of which reacts completely differently to machining. High tool wear and surface roughness are issues with AMMC machining that either render the procedure unworkable or result in an unprofitable manufacturing process (Bhardwaj *et al.*, 2020). Therefore, the geometry and wear resistance of the cutting tools, as well as the choice of ideal process settings, are subject to unique requirements when machining composite materials (Prakash & Krishnaraj, 2021; Zlámal *et al.*, 2018).

The ability of the fluid to lower the temperature produced by the frictional action between the cutting tool and the workpiece is the main benefit of wet machining (Zhou *et al.* 2015). As the temperature rises, the surface structure is impacted, increasing the workpiece's surface roughness (Pang *et al.* 2023). Thus, the fluid's impact will result in a decrease in the workpieces' surface roughness as well as a decrease in tool wear, extending the tool's lifespan (Tian *et al.* 2024; Kuram *et al.* 2024).

Eggshell composites' bioceramic qualities, sustainability, and capacity to improve mechanical performance have drawn a lot of interest in material science and machining (Admase *et al.*, 2025). Eggshell reinforcement shows promise in a variety of composite applications, particularly in machining operations where material hardness, wear resistance, and temperature stability are critical factors (Cunha *et al.*, 2019).

Eggshell-reinforced composites significantly increase tribological properties, compressive strength, and hardness in several investigations that looked at the mechanical behavior. Fillers made from eggshells increase thermal stability and flame retardancy, making them appropriate for applications requiring heat resistance (Cunha *et al.*, 2019; Hassen *et al.*, 2015). The effects of eggshell reinforcement on chip formation, built-up edge reduction, and material removal rate (MRR) in machining applications are demonstrated in conjunction with fly ash and carbonized eggshell matrix composites (Ononiwu *et al.*, 2021). The performance of eggshell-reinforced aluminum alloys has been improved in large part by optimizing machining parameters like depth of cut, feed rate, and cutting speed.

The innovation of Performance Optimization of Wet Turning of Aluminum Alloy 6351 Eggshell Reinforced Composite Using Response Surface Methodology (RSM) builds upon these findings by systematically analyzing the interaction between machining parameters and composite behavior. By employing RSM, researchers can refine machining conditions to achieve optimal surface roughness and material removal rates, ensuring efficient and sustainable machining practices.

3. METHODOLOGY

3.1. Materials

Figures 1 and 2 display the eggshells and eggshell powder respectively. The study employed various tools and materials, including a veneer caliper, measuring tape, aluminum alloy 6351, eggshell waste, surface tester (Mitutoyo SJ-210), and a CNC lathe machine (250 PCD Boxford CNC lathe machine) to achieve its objectives. Table 1 presents the chemical composition of the Al-6351 alloy, while Table 2 outlines its mechanical properties.

Figure 1. Egg shells

Figure 2. Egg shell powder

Table 1. Composition of the A6351 alloy

Al	Si	Fe	Cu	Mn	Mg	Zn	Ti	V
Bal	7.0	0.1	0.002	0.006	0.4	0	0.13	0.02

Table 2. Mechanical properties of Al-6351 alloy

Sample	Specimen	Toughness (Joules)	Hardness (BHN)
1	Al-6351	6.638	60

3.2. Methods

3.2.1. Aluminum alloy 6351 eggshell re-enforced composite preparation

The egg shells samples were gathered in large quantity, cleaned to get rid of dust and other debris, and then completely cleansed with water before being left to dry for an hour in an oven set to 1000°C (Nwoziri *et al.*, 2024). The dried egg shells were pulverized and crushed until they reached room temperature in order to get the finest crushed particle possible (Mba *et al.*, 2024; Nwoziri *et al.*, 2024). The extracted powder was passed through the proper size sieves (>106 to <850 microns) to produce particles with a consistent size distribution (Nwobi-Okoye & Uzochukwu 2020). The AAERCs consisted of 15% egg shell reinforcement and 85% aluminum alloy (Nwoziri *et al.*, 2024; Nwobi-Okoye *et al.*, 2019). The weights of the egg shell powder reinforcements were measured using an electronic compact scale (Mba *et al.*, 2024). A weighing balance was used to ascertain the weight of the aluminum that was supplied for the creation of AAERCs (Mba *et al.*, 2024). Wooden templates were utilized, and the sand mold was constructed using natural sand. The required amount of pulverized egg shell was kept warm in a furnace in order to improve wettability (Nwoziri *et al.*, 2024; Nwobi-Okoye *et al.*, 2019). The aluminum was firmly fastened using a temperature probe to ensure complete melting, which was necessary to create optimal strengthening when mixed with the pulverized dried egg shell (Nwoziri *et al.*, 2024). An electric-powered crucible furnace running on diesel was used to melt the aluminum alloy at a temperature

of 700°C ± 50°C (Nwoziri *et al.*, 2024). Aluminum was carefully placed within the furnace to cool and solidify into a semi-solid condition (Pola *et al.*, 2018). Magnesium powder (2%) was added to the molten metal in order to further boost the metal's wettability (Mba *et al.*, 2024; Nwoziri *et al.*, 2024). Reducing surface tension, increasing surface energy, and reducing matrix reinforcement interface energy are all achieved by obtaining the metals wettability (Ren *et al.*, 2024). The dried eggshell particles were added to the semi-solid melt at different temperatures and stirring intervals. After the mixture was superheated to 750°C ± 50°C, it was stirred using an automatic mechanical stirrer (Mishra & Tulasi 2020; Singh *et al.*, 2022). The fluid was then poured into a prepared sand mold and allowed to harden to make sound casts.

3.2.2. Design of experiment

The experimental design aimed to select machining settings in various combinations for 15 runs, incorporating three components and three levels. The goal was to identify the optimal input factors for the best response. Using the Box-Behnken design (BBD), the experiment included 15 runs with three components and three levels. Table 3 details the design levels and independent process variables.

Table 3. Independent process variable and design levels

Variables	Units	Low (-1)	Medium (0)	High (+1)
V_C	Rpm	180	450	720
F_r	mm/rev	0.2	0.3	0.4
D_C	Mm	0.2	0.4	0.6

3.2.3. Experimental set up

Orthogonal turning experiments were conducted using the versatile 250 PCD Boxford CNC lathe. The lathe's tool spindle moves linearly along the X, Y, and Z axes, making it ideal for this process. A cylindrical workpiece, approximately 220 mm in diameter and made of AAERC, was secured between the universal chuck's three jaws. The study focused on three main control variables: V_C, F_r and D_C. Experimental trials were performed with various combinations of these input variables. MRR and Ra values were meticulously recorded for each trial. Accurate input parameter entry is crucial to ensure the precision of the turning process model.

3.2.4. Cutting operation procedures

The AAERC was initially machined on a CNC lathe to achieve the required 22 mm diameter for each sample needed for the experimental inquiry following the DOE. The chuck was secured, and the workpiece was centered. The tool holder was equipped with an HSS cutting insert, and necessary adjustments were made before starting the machining process. Turning operations were initiated by combining the selected process control parameters using DOE. To determine the appropriate output values, turning was performed on AAERC using the input parameters specified by the DOE. A Mitutoyo SJ-210 surface roughness tester was used to measure Ra. Figures 3 and 4 depict the experimental CNC lathe setup and the machined sample of aluminum A6351 reinforced with eggshell, respectively.

Figure 3. Experimental setup (CNC lathe)

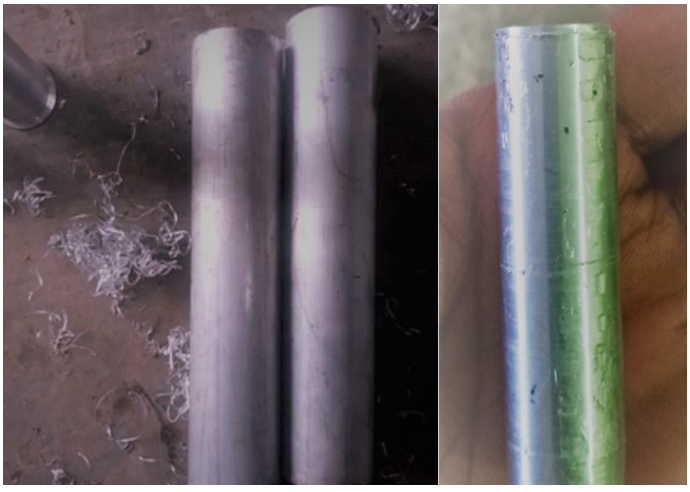

Figure 4. Al. A6351 Egg-shell machined sample

3.2.5. Surface roughness (SR) evaluation

Surface roughness, often referred to simply as roughness, is a key aspect of surface texture. It quantitatively measures the direction of the normal vector relative to the actual surface (Yu *et al.*, 2024). Surfaces with significant roughness variations are termed rough, while those with minimal variations are considered smooth. Understanding the frequency and amplitude of these fluctuations is essential to ensure the surface meets the intended application requirements. In this study, surface roughness for each experimental run was measured using a Mitutoyo surface measurement device. Figure 5 illustrates the Mitutoyo surface measuring instrument used for these measurements.

Figure 5. Mutotuyo surface measuring instrument

3.2.6. Metal removal rate (MRR) evaluation

Material Removal Rate (MRR) refers to the amount of material removed during machining over a specific period. It is calculated by dividing the weight of the workpiece by the machining time. The MRR equation was used to determine the material removal rate for each experimental run. Weighing machines were employed to measure the weight difference of the workpiece.

$$\text{MRR } (mm^3/min) = \frac{W_{bm} - W_{am}}{M_t}$$

W_{bm} = Workpiece weight before machining
W_{am} = Workpiece weight after machining
M_t = Total machining time for each trial (mins)

Material Removal Rate (MRR) significantly impacts CNC machining operations. Key effects include reduced lead times, faster material removal, shorter machining times, and increased productivity, all crucial for meeting production targets (Lu *et al.*, 2018). Lower MRR often results in smoother surface finishes, while higher MRR can cause increased vibrations and cutting forces, potentially leading to rougher surfaces (Azarhoushang & Kitzig-Frank 2022; Lin *et al.*, 2020). Higher MRR also generates more cutting forces, affecting the overall performance of the machining process, machine stability, and tool rigidity (O'Toole *et al.*, 2021). Additionally, higher MRR produces more heat at the cutting zone, necessitating effective heat management to prevent tool damage and workpiece distortion (Kumar & Singh 2020; Bijanzad *et al.*, 2022). Thicker chips are produced with higher MRR, requiring proper evacuation to avoid chip blockage and tool damage.

3.2.7. Cutting fluid evaluation

Applying high-pressure cutting fluid improves its penetration at the contact points between the tool and workpiece (Yan *et al.*, 2016). This technique enhances machining efficiency by reducing friction and dissipating heat from the cutting zone (Ashmawy *et al.*, 2023). High-pressure application significantly shortens contact length, minimizes tool wear, and improves surface smoothness (Wang *et al.*, 2022; Zhou *et al.* 2022). Filtering the cutting fluid is crucial to prevent microscopic particles from entering the high-pressure jet and affecting the workpiece's surface finish. High-pressure jet assistance (HPJA) effectively delivers cutting fluid, reducing cutting temperatures, pressures, and chip breakability while minimizing thermal stress buildup in both the tool and workpiece (Cica & Kramar 2019). In this study, Lubcon oil was used as the coolant for the machining process.

4. RESULTS AND DISCUSSION

The regulated parameters (V_C, F_r and D_C) and observed outcomes (MRR and Ra) for AAERC were optimized during the wet turning process using Response Surface Methodology (RSM). The optimization aimed to determine the best combination of input factors for optimal results. The ideal turning combination for AAERC and the desired response were identified using the numerical method in RSM. The regression model equation was derived by applying Equation 2, with the selected model based on the interaction of V_C, F_r and D_C. The input variables, in relation to each other, determine the individual response in terms of coded and actual variables as described in Equation 1.

$$y = f(x_1, x_2, x_3 \ldots x_k) \quad \ldots\ldots\ldots\ldots (1)$$

$$y = \beta_0 + \beta_1 x_1 + \beta_2 x_2 + \beta_3 x_3 + \beta_{123} x_1 x_2 x_3 + \varepsilon \quad \ldots\ldots\ldots\ldots (2)$$

Where;

$x_1 = V_C$, $x_2 = F_r$, and $x_3 = D_C$
y = Required output response (MRR and Ra).
f = Response function
ε = Random error (measurement error on response and background noise)
k is the number of independent variables.
β_0 is the intercept value of the variables
$\beta_1, \beta_2, \beta_3, \beta_{123}$ are coefficients associated with each variable and interaction of
$x_1, x_2, x_3, x_1 x_2 x_3$ respectively.

Table 4 presents the final design table after conducting the experiment by machining AAERC according to the DOE. The turning process utilized the necessary process variables to determine the required response values.

Table 4. Final data table of the actual design after experiment.

Runs	V_C	F_r	D_C	Ra	MRR
	(rpm)	(mm/min)	(mm)	(μm)	(mm^3/min)
1	450	0.3	0.4	1.28	1457.84
2	180	0.4	0.4	1.82	1386.1
3	450	0.2	0.6	1.22	2393.07
4	450	0.4	0.6	1.28	2091.48
5	180	0.3	0.6	2.61	2507.11

6	180	0.2	0.4	1.38	2639.45
7	720	0.3	0.2	0.61	518.31
8	180	0.3	0.2	1.32	1311.04
9	720	0.2	0.4	0.5	337.07
10	720	0.4	0.4	2.52	1322.35
11	450	0.4	0.2	1.82	726.58
12	720	0.3	0.6	0.14	869.35
13	450	0.2	0.2	0.62	1770.22
14	450	0.3	0.4	1.14	1396.84
15	450	0.3	0.2	1.02	722.89

4.1. Quantitative assessment of MRR using ANOVA

Table 5. ANOVA table of MRR

Source	Sum of Squares	df	Mean Square	F-value	p-value	
Model	7.356E+06	9	8.173E+05	21.22	0.0018	
V_C	3.121E+06	1	3.121E+06	81.04	0.0003	
F_r	1.431E+06	1	1.431E+06	37.17	0.0017	
D_C	1.981E+06	1	1.981E+06	51.44	0.0008	
$V_C \times F_r$	54772.38	1	54772.38	1.42	0.2865	significant
$V_C \times D_C$	1.785E+05	1	1.785E+05	4.64	0.0839	
$F_r \times D_C$	1.377E+05	1	1.377E+05	3.57	0.1173	
V_C^2	1.382E+05	1	1.382E+05	3.59	0.1167	
F_r^2	2.073E+05	1	2.073E+05	5.38	0.0681	
D_C^2	37159.38	1	37159.38	0.9649	0.3711	
Residual	1.926E+05	5	38510.96			
Lack of Fit	1.907E+05	4	47673.58	25.62	0.1470	not significant
Pure Error	1860.50	1	1860.50			
Cor Total	7.548E+06	14				

Table 5 presents the MRR ANOVA table, which evaluates the impact of the variables and their interactions on the response variable. The model is significant, as indicated by a p-value of 0.0018, meaning the variables in the model significantly affect MRR. A p-value of 0.1470 for the lack of fit suggests that the model fits the data well. The variables V_C, F_r and D_C have p-values of 0.0003, 0.0017, and 0.0008, respectively, indicating a significant effect on MRR.

Table 6. Fit statistics of MRR

Std. Dev.	196.24	**R^2**	0.9745
Mean	1416.65	**Adjusted R^2**	0.9286
C.V. %	13.85	**Predicted R^2**	0.7765
		Adeq Precision	13.7309

Table 6 presents the fit statistics for MRR. The high R^2 value of 0.9745 and adjusted R^2 of 0.9286 indicate that the model fits the data very well. The adequate precision ratio of 13.7309, which exceeds the benchmark of 4, signifies the model's effectiveness in navigating the design space. The difference between the adjusted R^2 of 0.9286 and the predicted R^2 of 0.7765 is less than 0.2, indicating satisfactory agreement. The standard deviation of 196.24 and coefficient of variation of 13.85 suggest

a moderate level of variability around the model's predictions. The model's significant ability to explain the variation in the dependent variable (MRR) and its sufficient precision enhance its predictability.

Table 7. Coefficients in terms of coded factors of MRR

Factor	Coefficient Estimate	df	Standard Error	95% CI Low	95% CI High	VIF
Intercept	1360.09	1	132.59	1019.25	1700.93	
V_c	-624.58	1	69.38	-802.93	-446.23	1.0000
F_r	-422.98	1	69.38	-601.33	-244.63	1.0000
D_C	475.48	1	66.30	305.06	645.90	1.02
$V_C \times F_r$	117.02	1	98.12	-135.21	369.25	1.0000
$V_C \times D_C$	-211.26	1	98.12	-463.49	40.97	1.0000
$F_r \times D_C$	185.51	1	98.12	-66.72	437.74	1.0000
V_C^2	-199.55	1	105.32	-470.29	71.19	1.08
F_r^2	244.33	1	105.32	-26.41	515.07	1.08
D_C^2	107.29	1	109.22	-173.48	388.06	1.12

Table 7 provides a detailed statistical summary of a regression model where the dependent variable is MRR (Material Removal Rate). A positive coefficient for D_C and the interaction between $F_r \times D_C$ indicates that as these factors increase, MRR also increases. Conversely, a negative coefficient for V_C, D_C, V_C^2 and $V_C \times D_C$ suggests that an increase in these factors leads to a decrease in MRR. The intercept, with a coefficient of 1360.09, represents the expected MRR in coded form when all factors are zero. The model appears to be free of significant multicollinearity, as indicated by the low VIF values of 1, ensuring the reliability of the coefficient estimates.

4.2. Coded equation

$MRR = +1360.9 - 624.58\ V_C - 422.98\ F_r + 475.48\ D_C + (117.02\ V_C \times F_r) - (211.26 V_C \times D_C) + (185.51\ F_r \times D_C) - 199.55 V_C^2 + 244.33\ F_r^2 + 107.29\ D_C^2$

The equation demonstrates how MRR is influenced by V_C, F_r and D_C. The exponents and coefficients indicate the sensitivity of MRR to changes in these parameters. Negative coefficients suggest that increasing these parameters individually decreases MRR, while the interaction term shows a positive effect, meaning the combined influence of these parameters increases MRR. The coded equation for MRR can be predicted by inputting the values for V_C, F_r and D_C. This equation simplifies the process of comparing and determining the relative importance of the component factors (V_C, F_r and D_C). Additionally, the scales and units for V_C, F_r and D_C can be easily adjusted using the coded equation, providing a consistent method for comparing the factors.

4.3. Actual equation

$MRR = +5786.84499 + 0.415038 V_C - 24550.31014 F_r - 790.60942 D_C + (4.33398 V_C \times F_r) - (3.91218 V_C \times D_C) + (9275.625 F_r \times D_C) - 0.002737 V_C^2 + 24433.23913 F_r^2 + 2682.27174 D_C^2$

The actual parameters measured during the turning process include V_C, F_r and D_C. The actual equation can be used to forecast the MRR once the real input values of V_C, F_r and D_C are known. This equation helps predict how different parameters affect the efficiency of MRR in CNC wet turning of AAERC, allowing for process optimization. The formula aids in optimizing the machining process by predicting MRR based on the input parameters. It shows how various parameters, such as V_C, F_r and D_C, impact MRR. A regression equation with a positive coefficient, quadratic effect, and interaction effect indicates that increasing the process parameters raises MRR, while a negative coefficient, quadratic effect, and interaction effect suggest that increasing the process parameters lowers MRR. The actual equation can be used to identify necessary adjustments when the response differs from the intended outcome. It quantifies the response sensitivity to input variables, guiding robust process designs.

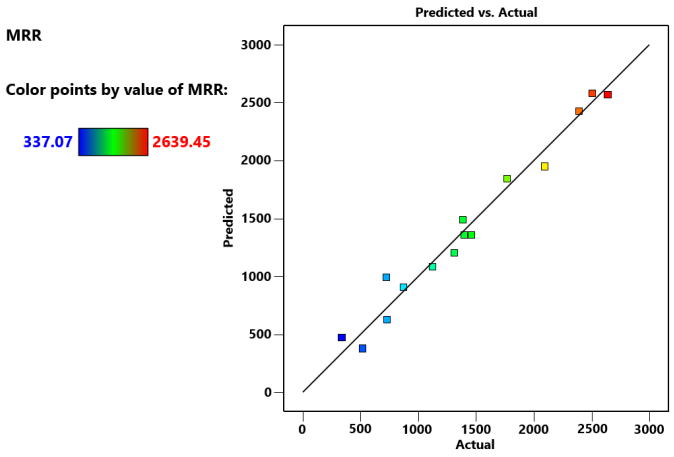

Figure 6. Graph of predicted values and actual values of MRR.

Figure 6 shows the graph of predicted versus actual MRR values. The predictive model is significant, as most data points are close to the diagonal line, indicating a strong correlation between predicted and actual MRR values. The proximity of each data point to the diagonal line underscores the model's significance. This model's importance enhances the optimization of process parameters for the best possible response.

4.4. Quantitative assessment of Ra using ANOVA

Table 8. ANOVA table of Ra

Source	Sum of Squares	df	Mean Square	F-value	p-value	
Model	5.30	9	0.5891	9.74	0.0110	
V_C	3.62	1	3.62	59.85	0.0006	
F_r	0.3613	1	0.3613	5.98	0.0583	
D_C	0.1331	1	0.1331	2.20	0.1980	
$V_C \times F_r$	0.0484	1	0.0484	0.8006	0.4119	significant
$V_C \times D_C$	0.7744	1	0.7744	12.81	0.0159	
$F_r \times D_C$	0.3249	1	0.3249	5.37	0.0682	
V_C^2	0.0298	1	0.0298	0.4925	0.5141	
F_r^2	0.0026	1	0.0026	0.0438	0.8425	
D_C^2	0.0140	1	0.0140	0.2317	0.6506	
Residual	0.3023	5	0.0605			
Lack of Fit	0.2925	4	0.0731	7.46	0.2672	not significant
Pure Error	0.0098	1	0.0098			
Cor Total	5.60	14				

Table 8 presents the ANOVA table for Ra, showing that the model has a p-value of 0.0110, indicating high significance and that the input variables significantly impact Ra. V_C and F_r are significant with p-values of 0.0006 and 0.0583, respectively. The non-significant lack of fit suggests an excellent fit between the model and the data. Table 9 displays the fit statistics for Ra, illustrating the model's strong fit with an R^2 value of 0.9271. The model's ability to explain the data is supported by the high R-squared value. The difference between the R^2 of 0.9461 and the adjusted R^2 of 0.8490 is less than 0.2, indicating satisfactory agreement. An R-squared value closer to 1, as seen with R^2 0.9461, indicates a better fit between the developed model and the gathered data. The R-squared values demonstrate the mathematical model's effectiveness in predicting the response. The high values of all determination coefficients confirm the strong correlation between the independent variables, highlighting the model's significance.

Table 9. Fit statistics of Ra

Std. Dev.	0.2459	**R^2**	0.9461
Mean	1.15	**Adjusted R^2**	0.8490
C.V. %	21.37	**Adeq Precision**	11.0830

Table 10. Coefficients in terms of coded factors of Ra

Factor	Coefficient Estimate	df	Standard Error	95% CI Low	95% CI High	VIF
Intercept	1.18	1	0.1661	0.7564	1.61	
V_C	-0.6725	1	0.0869	-0.8960	-0.4490	1.0000
F_r	0.2125	1	0.0869	-0.0110	0.4360	1.0000
D_C	0.1233	1	0.0831	-0.0903	0.3368	1.02
$V_C \times F_r$	-0.1100	1	0.1229	-0.4260	0.2060	1.0000
$V_C \times D_C$	-0.4400	1	0.1229	-0.7560	-0.1240	1.0000
$F_r \times D_C$	-0.2850	1	0.1229	-0.6010	0.0310	1.0000
V_C^2	-0.0926	1	0.1320	-0.4318	0.2466	1.08
F_r^2	-0.0276	1	0.1320	-0.3668	0.3116	1.08
D_C^2	0.0659	1	0.1369	-0.2859	0.4177	1.12

Table 10 presents the results of the analysis of variance, which indicates that the Ra mathematical models have the highest accuracy levels over the 95% confidence level, making them the most appropriate for response prediction. Table 10 explained the significance and dependability of each component in the regression model. The direction and strength of each factor's effect on Ra are shown by the coefficients. A negative coefficient indicates that increasing the coefficient of the corresponding parameter reduces the surface roughness. This suggests that the higher the coefficient of the corresponding parameter might lead to smoother surfaces. A positive coefficient indicates that increasing the coefficient of the corresponding parameter increases the surface roughness, implying rougher surfaces at higher coefficient of the corresponding parameter.

4.5. Coded equation

$Ra=+1.18-0.6725V_C+0.2125F_r+0.1233D_C-(0.1100V_C\times F_r)-(0.4400 V_C\times D_C)-(0.2825F_r\times D_C)-0.0926V_C^2-0.0276F_r^2+0.0659D_C^2$

Ra can be predicted provided the input variables (V_C, D_C, and F_r) in the equation have the necessary values. The application of the coded equation makes it easier and more convenient to evaluate the input variable coefficients, as well as to determine how the input and output interact.

4.6. Actual equation

$Ra=-2.54862+0.0031486V_C+11.31486\ F_r+7.24058\ D_C-(0.004074 V_C\times F_r)-(0.008148V_C\times D_C)-(14.25000F_r\times D_C)-1.27035^{-6}V_C^2-2.76087F_r^2+1.64674D_C^2$

The coefficients illustrate the links between each parameter and Ra as well as how they are affected. Ra is predictable if the input variables in the equation have the necessary values. The actual equation can be used to forecast the Ra when the genuine input values are available. These equations help with turning and machining process optimization for the composite by projecting Ra based on different input parameter values.

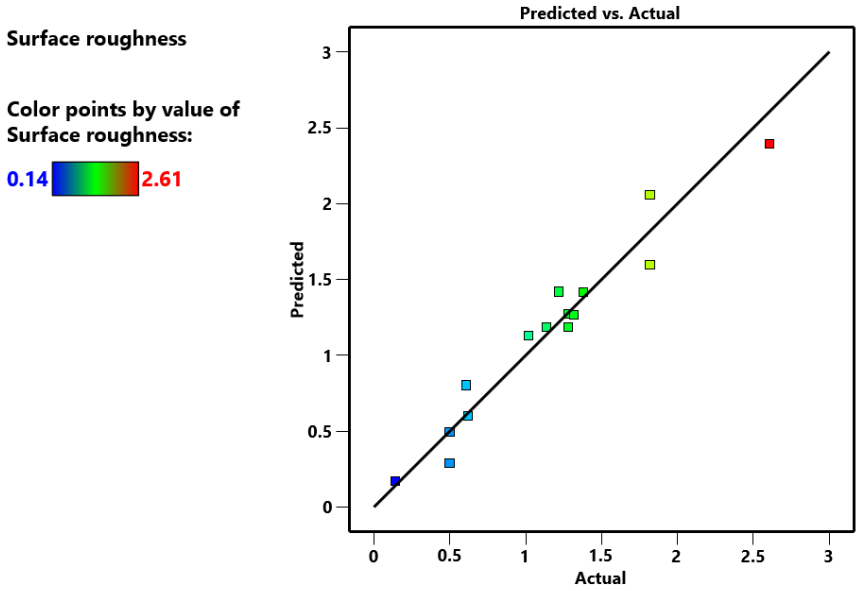

Figure 7. Graph of predicted values and actual values of Ra

Figure 7 shows the predicted value of Ra plotted against the actual value. The image shows a dispersed plot that compares the Ra's actual and predicted values. A line linking each point indicates the degree to which the actual and predicted values agree, and each point represents a pair of actual and predicted values. The points seem to follow the line of best fit quite closely, suggesting that the model's predictions are not too far off. A perfect prediction is shown as a diagonal line, where the predicted and actual values coincide exactly. The color-coded Scatter Points display a range of 0.14 (green) to 2.61 (red), according to the Ra. The diagonal line and the points are nearly in line with one another, suggesting that the predictive model does a good job of forecasting Ra.

4.7. Optimization utilizing numerical method

Figure 8 illustrates the numerical optimization of AAERC. The primary objective is to optimize Ra and MRR by selecting the ideal input variables. The optimization was conducted with a desirability function of 1. The study uses a numerical optimization technique to determine the best input combination for optimal response. The results indicate that the best values for Ra and MRR are 1.0689 μm and 1793.93 mm^3/min, respectively, when turning operations on AAERC are performed with input variables V_C, D_C, and F_r set at 369.822 rpm, 0.333554 mm/min, and 0.235944 mm, respectively.

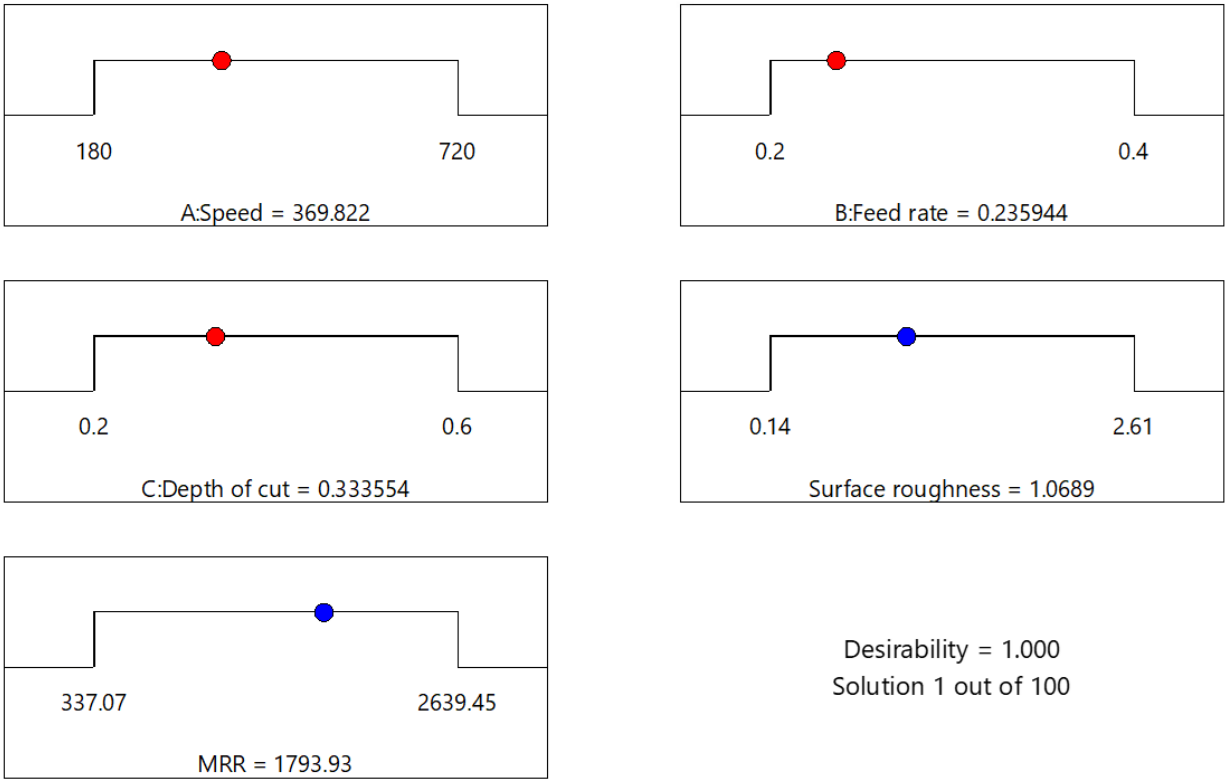

Figure 8. Numerical optimization of AAERC

The analysis demonstrates that the optimal outcome minimizes built-up edge development and improves chip flow, hence reducing surface roughness. Surface roughness and material removal efficiency are directly impacted by cutting speed, feed rate, and depth of cut because of the impacts of tool engagement (Truong *et al.*, 2025). Feed rate plays a crucial role in determining surface finish, as smaller incremental material removal results in smoother finishes, while excessive feed increases cutting forces, leading to rougher surfaces and potential tool deflection (Xu & Tang, 2014). Depth of cut affects material removal rate by controlling engagement volume, but excessive depths introduce instability and increased tool wear, impacting consistency in machining. The improved hardness and wear resistance of AAERC stabilizes machining performance, especially when turning in wet conditions. The eggshell reinforcement reduces thermal damage while preserving machining efficiency by promoting chip formation and aiding in heat dispersion (Gairola *et al.*, 2023; Guemmour *et al.*, 2015). High material removal efficiency and regulated surface finish are balanced by the interaction of process parameters, material qualities, and cutting mechanics, highlighting the significance of optimization in the machining of modern composites.

5. CONCLUSION

The objective of the wet turning of AAERC was to identify the optimal Ra and MRR in relation to three cutting parameters: V_C, F_r and D_C. The following conclusions were drawn from the evaluated findings:

The investigation successfully utilized AAERC. Response Surface Methodology (RSM) was employed to examine the interaction of input parameters with the response during the wet turning operation on AAERC. Numerical optimization was used to identify the optimal combinations of process parameters for achieving the best Ra and MRR outcomes.

The developed regression equation model can predict Ra and MRR when the values of input variables (V_C, F_r and D_C) are known. The parameters V_C, F_r and D_C significantly affect MRR, with p-values of 0.0003, 0.0017, and 0.0008, respectively. Similarly, V_C, and F_r significantly impact Ra, with p-values of 0.0006 and 0.0583, respectively.

The optimization results indicate that the best values for Ra and MRR are 1.0689 µm and 1793.93 mm³/min, respectively, when turning operations on AAERC are performed with input variables V_C, D_C, and F_r set at 369.822 rpm, 0.333554 mm/min, and 0.235944 mm, respectively.

This study is significant as it provides insights into the appropriate input parameters required to achieve the desired output parameters. Optimal selection of input variables reduces material waste, maximizes energy efficiency, and ensures the best surface finish.

Future research could concentrate on extending the use of AAERC in diverse machining operations and investigating how well it performs in various lubrication and cooling condition. Potential industry applications include aerospace, automotive, and precision manufacturing, although challenges such as high material costs, specialized equipment requirements, and process optimization may present barriers to widespread adoption.

ACKNOWLEDGMENT

The authors would like to extend their sincere gratitude to the

University of Calabar's Mechanical Engineering Department for their invaluable assistance in granting them access to the laboratory's supplies and equipment.

LIST OF ABBREVIATIONS

MRR	Material removal rate
AAERC	Aluminum alloy eggshell reinforced composite
AMMC	Aluminum metal matrix composites
BBD	Box-Behnken design
DOE	Design of experiment
Ra	Surface roughness
V_C	Cutting speed
D_C	Depth of cut
F_r	Feed rate
CNC	Computer numerical control
ANOVA	Analysis of Variance

REFERENCES

Abellán-Nebot, J. V., Vila Pastor, C., & Siller, H. R. (2024). A Review of the Factors Influencing Surface Roughness in Machining and Their Impact on Sustainability. *Sustainability, 16*(5), 1917. https://doi.org/10.3390/su16051917.

Admase, A. T., Eshetie, B. G., Asrade, E. D., & Gesese, T. N. (2025). *Evaluation of Sustainable Composite Materials Using Eggshell: Development and Characterization* (pp. 73–82). https://doi.org/10.1007/978-3-031-81730-4_6

Ashmawy, M., Elsheikh, A., & Elkassas, A. (2023). A review of cooling and lubrication techniques for machining difficult-to-cut material. *Journal of Engineering Research*, 7(1), 21–31. https://doi.org/10.21608/ERJENG.2023.183248.1134.

Azarhoushang, B., & Kitzig-Frank, H. (2022). Principles of grinding processes. In *Tribology and Fundamentals of Abrasive Machining Processes* (pp. 351–468). Elsevier. https://doi.org/10.1016/B978-0-12-823777-9.00001-X.

Bhardwaj, A. R., Vaidya, A. M., & Shekhawat, S. P. (2020). Machining of Aluminium Metal Matrix Composite: A Review. *Materials Today: Proceedings, 21*, 1396–1402. https://doi.org/10.1016/j.matpr.2020.01.179

Bijanzad, A., Munir, T., & Abdulhamid, F. (2022). Heat-assisted machining of superalloys: a review. *The International Journal of Advanced Manufacturing Technology, 118*(11–12), 3531–3557. https://doi.org/10.1007/s00170-021-08059-2.

Chen, J.-P., Gu, L., & He, G.-J. (2020). A review on conventional and nonconventional machining of SiC particle-reinforced aluminium matrix composites. *Advances in Manufacturing, 8*(3), 279–315. https://doi.org/10.1007/s40436-020-00313-2.

Cica, D., & Kramar, D. (2019). Multi-objective optimization of high-pressure jet-assisted turning of Inconel 718. *The International Journal of Advanced Manufacturing Technology, 105*(11), 4731–4745. https://doi.org/10.1007/s00170-019-04513-4.

Cunha, T. P., Siqueira, F. B., & Holanda, J. N. F. (2019). Development of Sustainable Eggshell Waste-Polyester Resin Composite Material for Using as Artificial Rock. *Materials Research, 22*(suppl 1). https://doi.org/10.1590/1980-5373-mr-2018-0865

Deresse, N. C., Deshpande, V., & Taifa, I. W. R. (2020). Experimental investigation of the effects of process parameters on material removal rate using Taguchi method in external cylindrical grinding operation. *Engineering Science and Technology, an International Journal, 23*(2), 405–420. https://doi.org/10.1016/j.jestch.2019.06.001.

Edh Mirzaei, N., Hilletofth, P., & Pal, R. (2021). Challenges to competitive manufacturing in high-cost environments: checklist and insights from Swedish manufacturing firms. *Operations Management Research, 14*(3–4), 272–292. https://doi.org/10.1007/s12063-021-00193-0.

Gairola, S., Sinha, S., & Singh, I. (2023). *Thermal and Flame Retardancy Behavior of Eggshell Filler Reinforced Polypropylene Composites* (pp. 201–206). https://doi.org/10.1007/978-981-99-1971-0_30

Gasha, S. B., Trautmann, M., & Wagner, G. (2024). Effect of Milling Time and Reinforcement Volume Fraction on Microstructure and Mechanical Properties of SiCp-Reinforced AA2017 Composite Powder Produced by High-Energy Ball Milling. *Materials, 17*(2), 435. https://doi.org/10.3390/ma17020435.

Guemmour, M. B., Sahli, A., Kebdani, S., & Sahli, S. (2015). Simulation of the Chip Formation and Temperature Distribution by the Fem. *Journal of Applied Sciences, 15*(9), 1138–1148. https://doi.org/10.3923/jas.2015.1138.1148

Guleria, V., Kumar, V., & Singh, P. K. (2023). *Recent Trends in the Amelioration and Prediction of Surface Roughness in Turning Process: A Bibliometric Analysis* (pp. 77–90). https://doi.org/10.1007/978-981-19-4208-2_7.

Hassen, A. A., Dizbay-Onat, M., Bansal, D., Bayush, T., & Vaidya, U. (2015). Utilization of Chicken Eggshell Waste as a Bio-Filler for Thermoplastic Polymers: Thermal and Mechanical Characterization of Polypropylene Filled with Naturally Derived CaCo 3. *Polymers and Polymer Composites, 23*(9), 653–662. https://doi.org/10.1177/096739111502300908

Jain, A., Kumar, C. S., & Shrivastava, Y. (2023). *Machining of Composite Materials Using Different Conventional and Unconventional Machining Processes: A Short Review* (pp. 75–83). https://doi.org/10.1007/978-981-19-1618-2_8.

Jain, P., Soni, S., & Baredar, P. (2014). Review on Machining of Aluminium Metal Matrix Composites. *Material Science Research India, 11*(2), 114–120. https://doi.org/10.13005/msri/110204

Jia, S., Wang, S., Lv, J., Cai, W., Zhang, N., Zhang, Z., & Bai, S. (2021). Multi-Objective Optimization of CNC Turning Process Parameters Considering Transient-Steady State Energy Consumption. *Sustainability, 13*(24), 13803. https://doi.org/10.3390/su132413803.

Jiang, X., Lu, W., & Zhang, Z. (2018). An approach for improving the machining efficiency and quality of aerospace curved thin-walled parts during five-axis NC machining. *The International Journal of Advanced Manufacturing Technology, 97*(5–8), 2477–2488. https://doi.org/10.1007/s00170-018-2129-0.

Jiang, Z., Chen, D., Sun, K., Pan, R., Fan, J., & Tang, Y. (2024). A systematic review of micro-texture formation based on milling: from mechanism, existing techniques, characterization to typical applications. *The International Journal of Advanced Manufacturing Technology, 134*, 2151–2177. https://doi.org/10.1007/s00170-024-14177-4.

Joshi, V., & Kumar, H. (2021). *Optimization of CNC Lathe Turning: A Review of Technique, Parameter and Outcome* (pp. 963–973). https://doi.org/10.1007/978-981-15-8542-5_85.

Kaniapan, K., Ali, M. A. M., Sulaiman, M. A., Minhat, M., & Aziz, M. S. A. (2022). *Review on Turning Process Parameters, Responses and Experimental Method of AISI 1045 Carbon Steel* (pp. 467–476). https://doi.org/10.1007/978-981-16-8954-3_44.

Karmiris-Obratanski, P., Thangaraj, M., Leszczyńska-Madej, B., & Markopoulos, A. P. (2024). Advanced Machining Technology for Modern Engineering Materials. *Materials, 17*(9), 2064. https://doi.org/10.3390/ma17092064.

Khan, F., Hossain, N., Mim, J. J., Rahman, S. M., Iqbal, Md. J., Billah, M., & Chowdhury, M. A. (2024). Advances of composite materials in automobile applications – A review. *Journal of Engineering Research.* https://doi.org/10.1016/j.jer.2024.02.017.

Kotteda, T. K., Kumar, M., Kumar, P., & Chekuri, R. B. R. (2022). Metal matrix nanocomposites: future scope in the fabrication and machining techniques. *The International Journal of Advanced Manufacturing Technology*. https://doi.org/10.1007/s00170-022-09847-0.

Krajčoviech, S., Holubjak, J., Richtarik, M., & Czánová, T. (2021). Identification of process Prime A turning when machining steel C56E2 and monitoring of cutting forces. *Transportation Research Procedia, 55*, 605–612. https://doi.org/10.1016/j.trpro.2021.07.027.

Kumar, A., Singh, V. P., Singh, R. C., Chaudhary, R., Kumar, D., & Mourad, A.-H. I. (2024). A review of aluminum metal matrix composites: fabrication route, reinforcements, microstructural, mechanical, and corrosion properties. *Journal of Materials Science, 59*(7), 2644–2711. https://doi.org/10.1007/s10853-024-09398-7

Kumar, R., Channi, A. S., Kaur, R., Sharma, S., Grewal, J. S., Singh, S., Verma, A., & Haber, R. (2023). Exploring the intricacies of machine learning-based optimization of electric discharge machining on squeeze cast TiB2/AA6061 composites: Insights from morphological, and microstructural aspects in the surface structure analysis of recast layer formation and worn-out analysis. *Journal of Materials Research and Technology, 26*, 8569–8603. https://doi.org/10.1016/j.jmrt.2023.09.127.

Kumar, S., & Singh, B. (2020). Stable Cutting Zone with Improved Metal Removal Rate in Turning Process. *Iranian Journal of Science and Technology, Transactions of Mechanical Engineering, 44*(1), 129–147. https://doi.org/10.1007/s40997-018-0253-y.

Kuram, E., Bagherzadeh, A., & Budak, E. (2024). Application of cutting fluids in micro-milling — A review. *The International Journal of Advanced Manufacturing Technology, 133*(1–2), 25–58. https://doi.org/10.1007/s00170-024-13752-z.

Li, H., Zhao, W., Gao, X., Shi, W., & He, N. (2024). Influence of cutting parameters on PCD tool wear during milling tungsten carbide. *The International Journal of Advanced Manufacturing Technology, 130*(3–4), 1165–1180. https://doi.org/10.1007/s00170-023-12775-2.

Li, X. F., Doh, S. I., Ramadhansyah, P. J., Hainin, M. R., & Mohd Haziman, W. I. (2021). *Effect of Eggshell Powder on the Mechanical and Durability Properties of Cement Mortar* (pp. 153–163). https://doi.org/10.1007/978-981-16-2187-1_14

Lin, Y.-C., Wu, K.-D., Shih, W.-C., Hsu, P.-K., & Hung, J.-P. (2020). Prediction of Surface Roughness Based on Cutting Parameters and Machining Vibration in End Milling Using Regression Method and Artificial Neural Network. *Applied Sciences, 10*(11), 3941. https://doi.org/10.3390/app10113941.

Lu, X., Zhang, H., Jia, Z., Feng, Y., & Liang, S. Y. (2018). Cutting parameters optimization for MRR under the constraints of surface roughness and cutter breakage in micro-milling process. *Journal of Mechanical Science and Technology, 32*(7), 3379–3388. https://doi.org/10.1007/s12206-018-0641-7.

Lv, J., Jia, S., Wang, H., Ding, K., & Chan, F. T. S. (2021). Comparison of different approaches for predicting material removal power in milling process. *The International Journal of Advanced Manufacturing Technology, 116*(1–2), 213–227. https://doi.org/10.1007/s00170-021-07257-2.

Maurya, R. K., & Niranjan, M. S. (2024). Optimization of Residual Stresses, Tool Wear, and Material Removal Rate of Tempered EN-36C Alloy Steel in CNC Turning Using Response Surface Methodology. *Journal of Materials Engineering and Performance, 33*(8), 3871–3884. https://doi.

org/10.1007/s11665-023-09053-3.

Mba, B., Nweze, N. C., Alozie, U., Onwuka, F., Omonini, C., & Nwoziri, S. C. (2024). The Performance Evaluation of Aluminum Alloy 356 Cow-Horn Composite as a Turning Machining Material Using Response Surface Methodology. *Journal of Basic and Applied Research International, 30*(5), 1–17. https://doi.org/10.56557/jobari/2024/v30i58842

Mishra, D., & Tulasi, T. (2020). *Experimental Investigation on Stir Casting Processing and Properties of Al 6082/SiC Metal Matrix Composites* (pp. 159–168). https://doi.org/10.1007/978-981-15-1124-0_14.

Mohanta, D. K., Sahoo, B., & Mohanty, A. M. (2024). Experimental analysis for optimization of process parameters in machining using coated tools. *Journal of Engineering and Applied Science, 71*(1), 38. https://doi.org/10.1186/s44147-024-00370-5.

Nwobi-Okoye, C. C., & Uzochukwu, C. U. (2020). RSM and ANN modeling for production of Al 6351/ egg shell reinforced composite: Multi objective optimization using genetic algorithm. *Materials Today Communications, 22*, 100674. https://doi.org/10.1016/j.mtcomm.2019.100674.

Nwobi-Okoye, C. C., Ochieze, B. Q., & Okiy, S. (2019). Multi-objective optimization and modeling of age hardening process using ANN, ANFIS and genetic algorithm: Results from aluminum alloy A356/cow horn particulate composite. *Journal of Materials Research and Technology, 8*(3), 3054–3075. https://doi.org/10.1016/j.jmrt.2019.01.031

Nwoziri, S. C., Mba, B., Onwuka, F., Agbonko, E. B., Alozie, U., Omonini, C., & Ogban-Ekpe, G. A. (2024). Assessment of Aluminum Alloy 6351 Eggshell Reinforced Composite in Dry Turning Using Response Surface Methodology. *Journal of Basic and Applied Research International, 30*(4), 43–60. https://doi.org/10.56557/jobari/2024/v30i48840

O'Toole, L., Kang, C.-W., & Fang, F.-Z. (2021). Precision micro-milling process: state of the art. *Advances in Manufacturing, 9*(2), 173–205. https://doi.org/10.1007/s40436-020-00323-0.

Ononiwu, N. H., Ozoegwu, C. G., Madushele, N., & Akinlabi, E. T. (2021). Machinability Studies and Optimization of AA 6082/Fly Ash/Carbonized Eggshell Matrix Composite. *Revue Des Composites et Des Matériaux Avancés, 31*(4), 207–216. https://doi.org/10.18280/rcma.310404

Pang, S., Zhao, W., Qiu, T., Liu, W., Yan, P., Jiao, L., & Wang, X. (2023). Effect of Cutting Fluid on Milled Surface Quality and Tool Life of Aluminum Alloy. *Materials, 16*(6), 2198. https://doi.org/10.3390/ma16062198.

Pawanr, S., & Gupta, K. (2024). Dry Machining Techniques for Sustainability in Metal Cutting: A Review. *Processes, 12*(2), 417. https://doi.org/10.3390/pr12020417.

Pola, A., Tocci, M., & Kapranos, P. (2018). Microstructure and Properties of Semi-Solid Aluminum Alloys: A Literature Review. *Metals, 8*(3), 181. https://doi.org/10.3390/met8030181.

Prakash, R., & Krishnaraj, V. (2021). *Cutting Tools for Machining Composites* (pp. 485–515). https://doi.org/10.1007/978-3-030-71438-3_18

Raja, V. K. B., & Gupta, M. (2021). Joining of Metal Matrix Composites. In *Encyclopedia of Materials: Composites* (pp. 502–511). Elsevier. https://doi.org/10.1016/B978-0-12-819724-0.00004-5.

Ren, J.-Y., Ji, G.-C., Guo, H.-R., Zhou, Y.-M., Tan, X., Zheng, W.-F., Xing, Q., Zhang, J.-Y., Sun, J.-R., Yang, H.-Y., Qiu, F., & Jiang, Q.-C. (2024). Nano-Enhanced Phase Reinforced Magnesium Matrix Composites: A Review of the Matrix, Reinforcement, Interface Design, Properties and Potential Applications. *Materials, 17*(10), 2454. https://doi.org/10.3390/ma17102454.

Seenath, A. A., & Sarhan, A. A. D. (2024). A State-of-the-Art Review on Cutting Tool Materials and Coatings in Enhancing the Tool Performance in Machining the Superior Nickel-Based Superalloys. *Arabian Journal for Science and Engineering, 49*(8), 10203–10236. https://doi.org/10.1007/s13369-024-08745-9.

Singh, A. K., Soni, S., & Rana, R. S. (2022). *Recent Trends on Furnace Design and Stirrer Blade Geometry Used in Stir Caster: A Focused Review* (pp. 147–159). https://doi.org/10.1007/978-981-16-5371-1_14.

Soni, D. L., Jagadish, & Neigapula, V. S. N. (2024). Tool surface texturing in machining performance: state of art and recent developments. *International Journal on Interactive Design and Manufacturing (IJIDeM), 19*, 1503-1531. https://doi.org/10.1007/s12008-024-01861-8.

Subbiah, S. (2014). Science of Machining. In *Handbook of Manufacturing Engineering and Technology* (pp. 1–21). Springer London. https://doi.org/10.1007/978-1-4471-4976-7_1-1.

Sun, W., Zhang, D., & Luo, M. (2021). Machining process monitoring and application: a review. *Journal of Advanced Manufacturing Science and Technology, 1*(2), 2021001–2021001. https://doi.org/10.51393/j.jamst.2021001.

Tefera, A. G., Sinha, D. K., & Gupta, G. (2023). Experimental investigation and optimization of cutting parameters during dry turning process of copper alloy. *Journal of Engineering and Applied Science, 70*(1), 145. https://doi.org/10.1186/s44147-023-00314-5.

Thanh, P. D., Long, B. T., & Hoa, P. T. (2024). *Research on Cutting Parameters Affecting Material Removal Efficiency and Surface Roughness When Turning of C3604 Copper* (pp. 115–122). https://doi.org/10.1007/978-3-031-39090-6_13.

Tian, C., Jiang, H., Yuan, S., Deng, J., & Yue, X. (2024). Research on cutting performance and processing surface quality of micro-structured composite-coated tool: a comprehensive

review. *The International Journal of Advanced Manufacturing Technology, 133*(5–6), 2709–2743. https://doi.org/10.1007/s00170-024-13908-x.

Tiwari, S., & Yadav, R. K. (2024). *Mechanical and Tribological Properties of Aluminum Metal Matrix Composites—A Review* (pp. 147–156). https://doi.org/10.1007/978-981-97-4947-8_13

Truong, H.-S., Nguyen, T.-T., & Bui, T.-A. (2025). *Evaluating the Impact of Cutting Speed and Feed Rate on Surface Roughness Utilizing a Four-Insert Carbide Face Milling Cutter on CNC Machines* (pp. 347–356). https://doi.org/10.1007/978-981-97-7083-0_34

Udaya Prakash, J., Sarala Rubi, C., Palani, S., Jebarose Juliyana, S., & Divya Sadhana, A. (2022). Optimization of machining parameters in drilling of LM6/B 4 C/Fly ash hybrid composites. *Manufacturing Review, 9*, 28. https://doi.org/10.1051/mfreview/2022026.

Wang, J., Gao, Q., Lu, J., Zheng, Q., Xi, X., Zhang, Y., & Zhao, W. (2024). Fast ED-milling of high-volume fraction Al/SiCp metal matrix composites. *CIRP Annals, 73*(1), 121–124. https://doi.org/10.1016/j.cirp.2024.03.014.

Wang, R., Yang, D., Wang, W., Wei, F., Lu, Y., & Li, Y. (2022). Tool Wear in Nickel-Based Superalloy Machining: An Overview. *Processes, 10*(11), 2380. https://doi.org/10.3390/pr10112380.

Wong, W. L. E., & Seetharaman, S. (2021). *Metal Matrix Composites* (pp. 129–158). https://doi.org/10.1007/978-3-030-71438-3_6.

Xu, K., & Tang, K. (2014). Five-axis tool path and feed rate optimization based on the cutting force–area quotient potential field. *The International Journal of Advanced Manufacturing Technology, 75*(9–12), 1661–1679. https://doi.org/10.1007/s00170-014-6221-9

Yan, P., Rong, Y., & Wang, G. (2016). The effect of cutting fluids applied in metal cutting process. *Proceedings of the Institution of Mechanical Engineers, Part B: Journal of Engineering Manufacture, 230*(1), 19–37. https://doi.org/10.1177/0954405415590993.

Yan, T., Qiu, B., Yuan, J., Pavesi, G., Zhao, F., & Wang, H. (2023). Flow State at Impeller Inlet: Optimization of Conical Frustum Section of Elbow Inlet Conduit in Large Low-Lift Pump Station. *Journal of Fluids Engineering, 145*(4). https://doi.org/10.1115/1.4056452.

Yu, X., Li, Z., Sheng, W., & Zhang, C. (2024). A new surface roughness measurement method based on QR-SVM. *The International Journal of Advanced Manufacturing Technology, 133*(7–8), 3987–3997. https://doi.org/10.1007/s00170-024-13898-w.

Zheng, L., Chen, W., & Huo, D. (2020). Review of vibration devices for vibration-assisted machining. *The International Journal of Advanced Manufacturing Technology, 108*(5–6), 1631–1651. https://doi.org/10.1007/s00170-020-05483-8.

Zhou, Y., Liu, C., Yu, X., Liu, B., & Quan, Y. (2022). Tool wear mechanism, monitoring and remaining useful life (RUL) technology based on big data: a review. *SN Applied Sciences, 4*(8), 232. https://doi.org/10.1007/s42452-022-05114-9.

Zhou, Y., Zhu, H., Zhang, W., Zuo, X., Li, Y., & Yang, J. (2015). Influence of surface roughness on the friction property of textured surface. *Advances in Mechanical Engineering, 7*(2), 168781401456850. https://doi.org/10.1177/1687814014568500.

Zlámal, T., Hajnyš, J., Petrů, J., & Mrkvica, I. (2018). Effect of the Cutting Tool Geometry on the Tool Wear Resistance when Machining Inconel 625. *Advances in Science and Technology Research Journal, 12*(1), 236–243. https://doi.org/10.12913/22998624/86262